Phys. Status Solidi C 7, No. 3–4, 1061–1064 (2010) / DOI 10.1002/pssc.200982858

physica status solidi c
www.pss-c.com
current topics in solid state physics

Amorphous silicon thin-film solar cells deposited on flexible substrates using different zinc oxide layers

P. Alpuim[*,1], A. Samantilleke[1], E. Marins[1], F. Oliveira[1,#], M. F. Cerqueira[1,#], L. Rebouta[1], S. Stefanov[2], S. Chiussi[2], C. Serra[2#], and J.E. Bourée[3]

[1] Centro de Física, Universidade do Minho, 4800-058 Guimarães, [#]4710-057 Braga, Portugal
[2] Departamento de Física Aplicada, E.T.S.I.Industriales, [#]C.A.C.T.I., Universidade de Vigo, Campus Universitario Lagoas Marcosende, 36310 Vigo, Spain
[3] Laboratoire de Physique des Interfaces et des Couches Minces, CNRS UMR 7647, Ecole Polytechnique, 91128 Palaiseau, France

Received 2 August 2009, revised 7 October 2009, accepted 28 October 2009
Published online 3 March 2010

PACS 52.50.Jm, 73.50.-h, 81.05.Gc, 81.15.Gh, 84.60.Jt

* Corresponding author: e-mail palpuim@fisica.uminho.pt, Phone: +351 510 463, Fax: +351 510 461

In order to improve the transparent contact layer in amorphous silicon solar cells fabricated on low-temperature plastic substrates, Al and Ga doped ZnO films were deposited at room temperature on plastic and glass and their optical, electronic and structural properties were correlated and optimized. Aiming to explore light trapping effects, plastic substrates were laser textured and their haze and total transmittance and reflectance were compared with those of untextured substrates. Although the haze increased dramatically, from 1.7 to 78.9 %, the total transmittance of PET coated with ZnO:Ga decreased from 83.9 %, in the untextured substrate, to 58.5 % in the textured PET. The haze in reflected light of PET coated with Al increased from 4.3% to 66.2% after texturing but the total reflectance decreased from 70.1 % to 36.8 %. Therefore the untextured substrates were used in the solar cells. a-Si:H solar cells were deposited at a substrate temperature of 150ºC on plastic, in the superstrate p-i-n configuration, and on stainless steel, in the substrate n-i-p configuration. The efficiency is ~5% in both types of devices, limited by low J_{sc} and low fill factor.

1 Introduction Solar cells fabricated with hydrogenated amorphous silicon (a-Si:H) absorbers are a leading thin-film, low-cost alternative to those made with bulk crystalline silicon. The large optical absorption coefficient across the solar spectrum means, an absorber layer of thickness less than 500 nm of a-Si:H is sufficient for an efficient solar cell operation. However, in practice, the absorber layer thickness is made even lower (~ 300 nm) because of the limited minority carrier diffusion length (<100 nm) as a result of the intra-bandgap density of states typical of a-Si:H. Hence alternative technological steps are being studied in order to improve the efficiency of the cell while reducing the cost-per-peak watt.

One such cost cutting step is the use of flexible substrates, which can be used in roll-to-roll production, replacing traditional glass substrates. However, the challenge of depositing thin-film silicon cells on plastic substrates is intrinsically linked to the maximum temperature that these substrates can endure. Unfortunately, the critical temperatures related to these two technologies (plastics and a-Si:H) make their simultaneous use difficult, as the properties of amorphous silicon degrade dramatically when deposited near the softening temperatures of plastics. For example, the dangling bond density of a-Si:H increases by an order of magnitude for each 50°C when descending below 200 °C [1]. In addition to dangling bonds, the low temperature deposition induces other macroscopic defects such as elongated voids and columnar amorphous growth [2]. The use of hydrogen dilution of silane partially compensates for the low substrate temperature [1-4]. This is due to the hydrogen passivation of dangling bonds, to the local heating provided by the exothermic reaction of H_2 evolution

from the growing film surface, and to the formation of a more relaxed amorphous structure. Stainless steel (SS) is an alternative flexible substrate with high temperature tolerance. SS has been used successfully as a substrate at low temperature (<150 ºC) [4]. In this work, a-Si:H thin films are deposited in a parameter range that yields amorphous silicon close to the onset of the amorphous-to-microcrystalline phase transition on plastic and SS substrates at 150 ºC.

Another issue for fabrication on plastics is the deposition of the transparent and conductive oxide (TCO) used as contact window layer in a-Si:H solar cells. These layers are typically made on glass, at high temperature (>150 ºC) and often employing wet chemistry for surface texturization that are not compatible with plastic substrates [3]. In this work doped zinc oxide is deposited at room temperature directly on plastic, for superstrate devices, or on top of the semiconductor stack, for substrate devices. Al and Ga are used as dopants and their effect on the structural, optical and electronic properties of the TCO are studied.

In order to increase the relatively low efficiency of a-Si:H solar cells it is crucial to develop light-trapping schemes that largely increase the optical path length inside the absorbing layer [5]. Excimer laser texturization of plastic substrates was carried out and the resulting optical characteristics of the substrates are reported.

2 Experimental ZnO:Ga (GZO) and ZnO:Al (AZO) thin films were deposited at room temperature in a vacuum under a Ar atmosphere with a base pressure of 2×10^{-6} Torr by dc magnetron sputtering keeping a target-to-substrate distance constant at 8 cm in all runs. For GZO deposition a 2-inch ZnO:Ga target, (zinc oxide/gallium, 95.5/4.5 wt.%), a working pressure of 4 mTorr, a target current density of 4.9 mA cm^{-2} has been used and a deposition rate of 0.47 nm/s was obtained. For AZO deposition a 4-inch ZnO:Al target, (zinc oxide/aluminium, 98.0/2.0 wt.%), a working pressure of 3 mTorr, a target current density of 2.5 mA cm^{-2} has been used and a deposition rate of 0.48 nm/s was obtained. X-ray diffraction (XRD) was used to examine the texture using Cu Kα radiation. (Bruker AXS Discover D8 apparatus).

The texturing of plastic substrates, consisting of ablation at laser radiation above the material damage threshold, was performed on polyester films (polyethylene terephthalate, PET) with thickness 125 µm. Substrates were cleaned in ethanol in an ultrasonic bath for 10 min followed by 10 min in water. The light source was ArF Excimer Laser (193 nm). Fluence was controlled by an attenuator (Lasoptics) followed by imaging using a fly's eye homogenizer (EX-HS-700D) with 650 mm spherical focusing lens. The sample was positioned on a holder with single axis servo motor at the focus of the homogenizer allowing movement in direction perpendicular to the incident beam. Laser repetition rate was always 1 Hz, fluence was varied as follows: 50, 60 and 70 mJ/cm^2, with the corresponding velocity 0.5, 0.5 and 1 mm/s. Optical properties of the textured plastics substrates were measured in a Shimadzu spectrophotometer in transmission and reflection modes.

Flexible SS substrates were mechanically polished and cleaned by ultrasonication followed by rinsing in deionised water and isopropanol. The rms roughness Δ_{rms} of SS substrates decreased from 430 nm to 80 nm on average, after polishing. A 250 nm thermally evaporated Al layer or a DC sputtered Cr layer was used as back reflective contact. After Al evaporation the SS substrate showed a Δ_{rms} of 60 nm. A thin (~30 nm) GZO (5.1 Ω/sq sheet resistance and 80% transmittance in the visible region) was DC sputtered directly on the SS/Al(or Cr) substrates prior to solar cell fabrication. Finally, a thicker GZO layer (700 nm) was deposited as the front contact to complete the substrate solar cell. For some cells, a SiN_x adhesion layer was deposited by Hot-wire CVD on SS before the Al deposition. The area of the solar cells, defined by the area of the ZnO:Ga front contact, was 0.126 cm^2 or 0.0314 cm^2. Selected solar cells were annealed at 150 ºC in vacuum for one hour.

Single junction p-i-n superstrate solar cells were fabricated at 150ºC on plastic by rf-PECVD using hydrogen dilution of silane, as described in ref. [12].

3 Results and discussion

3.1 Doped ZnO films Figure 1 shows the Raman spectra of ZnO films of thickness ~700 nm doped with Al (top) and with Ga (bottom). The optical transmittance was >80 % in both films. The Raman characteristic 437 cm^{-1} peak of ZnO wurtzite structure, assigned to the non-polar optical phonon mode (*E*2-high) is present in both spectra. Likewise, a broad band in the spectral region close to the LO phonon frequencies of undoped c-ZnO (574 cm^{-1} for A1-mode and 583 cm^{-1} for E1-mode [6]) is well defined, though its profile and maximum peak position changes with the dopant ion. These modes are ascribed to defects of oxygen vacancies and interstitial Zn and free carriers [7].

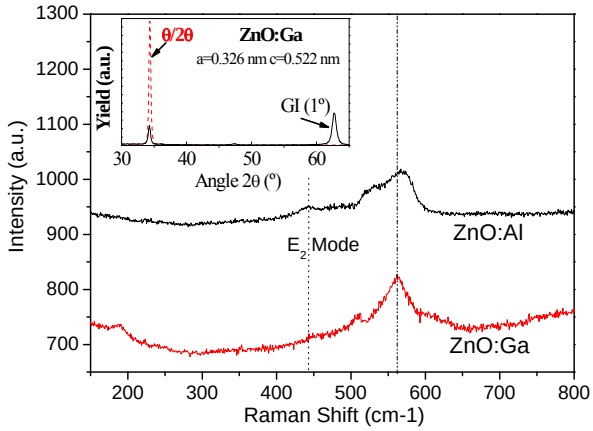

Figure 1 Raman spectra of ~700 nm thick Ga (bottom) and Al (top) doped ZnO films. The inset shows the XRD diffractogram of the ZnO:Ga film taken in the θ/2θ (dashed line) and in the grazing incidence (θ=1º) geometries.

It is known that most undoped ZnO material is strongly *n*-type. It has long been assumed that the dominant donor is a native defect, either the O vacancy V_O, or the Zn interstitial Zn_I [8]. Since the *A*1–LO-Raman mode of ZnO is related to the formation of the oxygen deficiency, interstitial zinc and free carrier [9], the low resistivity of the GZO and AZO thin films obtained in the present work (8.8×10^{-4} Ω cm and 2.6×10^{-3} Ω cm, respectively) is ascribed to the high concentration of V_O, or/and Zn_I. It may be interesting to note that in spite of the low crystalline fraction of the ZnO:Ga sample deposited at RT (due to the small amplitude of the E2 high mode) an extra mode at 510 cm^{-1} is present. This extra peak has no clear assignment. In ref.[10] the appearance of three new Raman modes at 512, 594, and 639 cm^{-1} in the Ga doped samples is observed and is consistent with previous experimental results on GZO thin films [6]. In Fig. 1, the presence of this mode in the ZnO:Ga spectrum and its absence from the ZnO:Al spectrum, support the hypothesis that it is due to the differences in mass and ionic radii between Ga and the host Zn atoms.

The inset in Fig. 1 shows the XRD data of ZnO:Ga, performed under θ/2θ geometry and also using grazing incidence (1º). The diffractogram of ZnO:Al film (not shown) is very similar. The ZnO:Ga films are textured, with the c-axis perpendicular to the substrate surface. The (002) diffraction peak is slightly shifted to a higher θ angle. The lattice *c* parameter is slightly higher and *a* is slightly lower than the correspondent in standard ZnO file (PDF -036-1451). This can be justified by the presence of a small compressive residual stress in the film. The average crystallite size has been estimated by means of Fourier analysis and is about 20 nm.

3.2 Laser texturing of PET substrates Figure 2 shows the transmittance of scattered light, in the optical wavelengths, of 125 μm thick PET substrates covered with ~700 nm of ZnO:Ga. Some substrates were laser treated, previously to ZnO deposition, using different irradiation conditions, summarized in Table 1. The transmittance data of flat, uncoated PET is included in Fig. 2, for comparison. The total transmittance (inset) of the untreated PET/GZO substrates is very high, close to that of uncoated PET, except for the displacement to slightly higher wavelengths of the absorption edge in the GZO coated substrates. It can also be seen that haze, defined as the ratio between the transmitted (or reflected) scattered light and the total transmitted (reflected) light, increases from 1.5% in the as deposited PET/GZO substrate to ~ 40% in the PET/GZO substrate treated with a laser fluence of 50 mJ/cm^2. The maximal scattered transmittance is found at around 550 nm, which closely matches the maximum of the solar spectrum. However, the total transmittance data (see inset) reveals that the laser treated substrates are less transparent than untreated ones. The scattered reflectance of Al-coated PET substrates increased from ~3% in untreated PET to 30% at

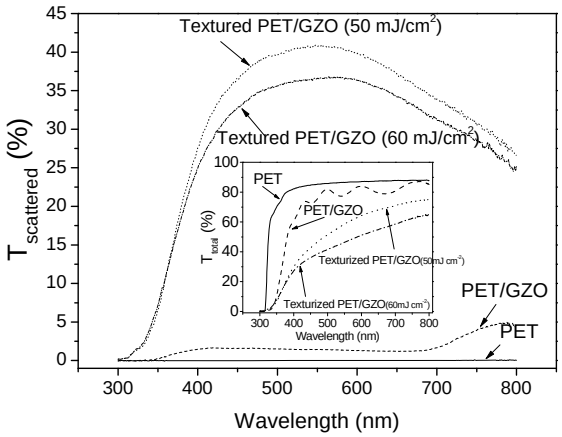

Figure 2 Transmittance of scattered light by 125 μm thick PET substrates covered with ~700 nm of ZnO:Ga. Two of the substrates were laser textured using fluences of 50 and 60 mJ/cm^2 before GZO deposition. The transmittance of a bare PET substrate is given for comparison. Inset shows the specular transmittance for the same group of samples.

550 nm on Al-coated laser textured PET substrates, using a fluence of 60 mJ/cm^2. However, the total reflectance (scattered + specular) decreased from 70% to ~30%.

Table 1 PET substrate roughness after laser irradiation.

Energy (mJ/cm^2)	Velocity (mm/s)	RMS roughness, R_a (nm)	
		uncoated	Al-coated*
70	1	31.7	71.4
60	0.5	26.1	111.2
50	0.5	53.5	102.5

* 183 nm thick.

3.3 Solar cells As-deposited solar cells showed conversion efficiency (η) between 1-3% under AM 1.5 conditions. Upon annealing at 150ºC for 30 min to 1 hour in vacuum, conversion efficiency improved. Figure 3 compares current – voltage (J-V) characteristics of p-i-n solar cells in superstrate configuration deposited on plastic (SC88 and SC94) and a n-i-p substrate solar cell deposited on SS (SC110) at 150 ºC. The cells SC88 and SC110 have 9 nm and 5 nm thick, respectively, high bandgap a-Si:H buffer layer in the i/p interface. The parameters derived from the J-V plot are given in Table 2. In the absence of light trapping schemes, the solar cell with the thicker absorber layer (SC88) showed the highest short-circuit current density (J_{sc}) and η. The increase in J_{sc} upon annealing is mainly responsible for the observed increase in the solar cell efficiency. Some dopant activation in the p-layer and defect annealing in the i-layer and at the interfaces could explain the observed increase in the open circuit voltage (from 0.77 V to 0.82 V in the case of SC110) after annealing.

A good adhesion was observed between Cr and SS as well as between Cr and n-a-Si:H with no SiN_x intermediate layer,

unlike in the case of Al. However, a notable difference in efficiency was not observed when using Al or Cr back contatcs.

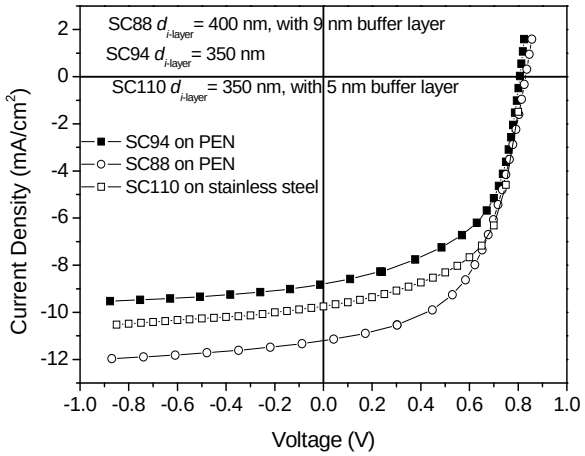

Figure 3 AM1.5 *I-V* curves of solar cells n-i-p deposited on SS (SC110, open squares), and p-i-n (SC88, open circles, SC94, solid squares) deposited on plastic (PEN).

Spectral Response (SR) measurements were carried out under zero bias and a small reverse bias, in order to evaluate the charge collection and loss mechanism of the solar cells. Figure 4 shows the external quantum efficiency (EQE) as a function of photon wavelength (λ), derived from SR results of annealed solar cells.

The EQE of a calibrated solar cell (R-SC) deposited on ITO/Glass substrate at 250 ºC is also plotted as a reference. It is apparent that one main difference between the R-SC and the flexible solar cells is the response in the long wavelength part of the spectrum, which could be explained by a reduced hole mobility and a non-regulated light trapping mechanism in the flexible solar cells. The drop in maximum EQE from 0.71 in the R-SC to 0.64 and 0.53 in the flexible solar cells is primarily due to enhanced recombination in the i-layer.

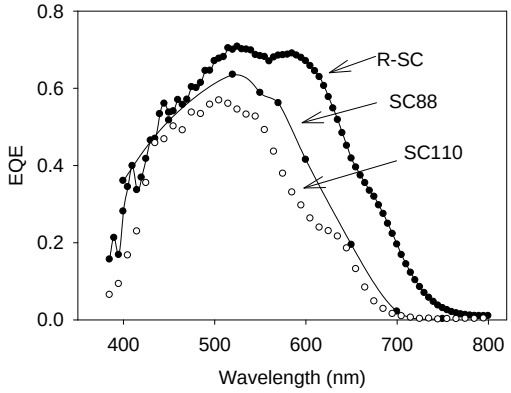

Figure 4 EQE under zero bias of a-Si:H solar cells deposited on SS and PEN substrates.

The relatively high EQE of the R-SC at short λ end of the spectrum suggests that the bandgap of p-layer in flexible solar cells has to be increased for the window layer to become more transparent in the UV and for better charge collection efficiency. The difference in EQE, between SC110 (on SS) and SC88 (on PEN) is attributed to the improved back reflector on PEN and the thicker absorber layer in the SC88 (Ref. [2]).

Table 2 Summary of electrical characteristics of solar cells.

Cell	Voc (V)	J_{sc} (mA/cm^2)	FF	η (%)
SC94	0.806	8.80	55.1	3.91
SC110	0.820	9.75	56.2	4.66
SC88	0.830	11.2	54.2	5.03

4 Conclusions In this work, plastic superstrate p-i-n and stainless steel substrate n-i-p solar cells were fabricated with efficiencies 5 and ~ 4.5%, respectively. These efficiencies are limited by J_{sc} and FF with the highest η coming from cell with the thickest (400 nm) absorber layer. Solar cell characteristics observed were similar for cells with Cr and Al back reflectors.

Laser texturing of plastic substrates increased dramatically the scattered transmittance (from 1.5 to >40%) and scattered reflectance (from 3 to 30%). However, the total transmittance and total reflectance decreased markedly in both cases.

ZnO films doped with Ga and Al were deposited at room temperature on PEN and PET substrates with optical transmittance in the visible ~80%. The resistivity of ZnO:Ga films is 8.8×10^{-4} Ω cm and that of ZnO:Al is 2.6×10^{-3} Ω cm. Films are polycrystalline with a low crystalline fraction. The correlation between structure and conductivity was made for Ga and Al doped ZnO films.

Acknowledgements This work was supported by Fundação para a Ciência e Tecnologia (FCT) through Pluriannual Contract with CFUM and FCT/CNRS bi-lateral project n°20798.

References

[1] P. Alpuim, V. Chu, and J. P. Conde, J. Appl. Phys. **86**(7), 3812 (1999).
[2] M. Brinza, J.K. Rath, and R.E.I. Shropp, Sol. Energy Mater. Sol. Cells **93**, 680 (2009).
[3] W. Beyer, J. Hüpkes, and H. Stiebig, Thin Solid Films **516**, 147 (2007).
[4] S. Guha, J. Yang, D.L. Williamson, Y. Lubianiker, J.D. Cohen, and A.H. Mahan, Appl. Phys. Lett. **74**(13), 1860 (1999).
[5] J. Escarre et al., Sol. Energy Mater. Sol. Cells **87**, 333 (2005).
[6] C. Bundesmann et al., Appl. Phys. Lett. **83**(10), 1974 (2003).
[7] J.M. Calleja and M. Cardona, Phys. Rev. B **16**, 3753 (1977).
[8] G. Heiland et al., in: Solid State Physics, ed. by F. Seitz and D. Turnbull (Academic, New York, 1959), Vol. 8, p. 191.
[9] S.K. Sharma and G.J. Exarhos, Solid State Phenom. **55**, 32 (1997).
[10] M. Snure and A.Tiwari, J. Appl. Phys. **104**, 073707 (2008).

